J Therm Anal Calorim (2012) 107:1177–1189
DOI 10.1007/s10973-011-1959-x

Devolatilization non-isothermal kinetic analysis of agricultural stalks and application of TG-FT/IR analysis

Aysel Kantürk Figen · Osman İsmail · Sabriye Pişkin

Received: 25 September 2010 / Accepted: 26 September 2011 / Published online: 8 October 2011

Abstract Devolatilization behavior of several types of agricultural stalks (sunflower, rice, corn, and wheat) was studied using thermogravimetric system (TG) under nitrogen atmosphere at different heating rates (10, 15, and 20 °C min^{-1}). Coats&Redfern, Horowitz&Metzger, and Arrhenius non-isothermal kinetic models were applied to calculate the devolatilization kinetic parameters and the devolatilization rate equations have been established. In addition, the kinetic compensation effect (KCE) has also been used to correlate pre-exponential factor (k_o) with activation energy (E_a) and an existence of the KCE is accepted. TG-FT/IR analyses were applied of the different stalks and FT/IR stack plot used to analyze the devolatilization gas products (CO_2, CH_4, HCOOH, CH_3OH). Infrared vibrational frequencies, micro structure and crystallinity of stalks were investigated by Fourier transform infrared spectroscopy (FT/IR), scanning electron microscope (SEM), and X-ray diffraction analysis (XRD), respectively.

Keywords Devolatilization · Agricultural stalks · Coats & Redfern · Horowitz&Metzger · Arrhenius · TG-FT/IR · Kinetic compensation effect

A. K. Figen · O. İsmail · S. Pişkin (✉)
Department of Chemical Engineering, Yildiz Technical University, Davutpasa Campus, N.127, Esenler, Istanbul, Turkey
e-mail: piskin@yildiz.edu.tr

A. K. Figen
e-mail: akanturk@yildiz.edu.tr

O. İsmail
e-mail: ismail@yildiz.edu.tr

Introduction

Lignocellulosic materials such as agricultural residues, wood, and food processing wastes are considered as low cost and abundant raw materials for several industries. They could be optimized to produce the corresponding products, such as liquid fuels and syngas, even high quality chemicals. Especially, they are considered a sustainable energy source as replacement for fossil fuel. Residual biomasses were studied because their availability is the best-accepted solution for the possible problems related to the competition of bio-fuels and food [1, 2]. Due to differences in chemical and physical properties of the sources, replacing coal means that the combustion and pyrolysis behavior is the main issue must be considered. In all cases, a fundamental characterization is required for these types of fuels which exhibit very different properties. After the devolatilization of agricultural biomaterials; include hemicellulose, cellulose and lignin; each fuel species is converted via two competing reactions into gasses and char. The devolatilization behavior of biomass materials has often been validated with thermogravimetric (TG) analysis and also evolving in the pyrolysis of biomass fuels has been studied with TG analysis coupled with Fourier transformed infrared (FT/IR). It was reported the TG-FT/IR pyrolysis experiment at low heating rates of biomass samples (wheat straw, tobacco) and pyrolysis yield was evaluated [3]. It was investigated palm oil waste, are the major agricultural wastes in countries in southeast Asia, pyrolysis means of TG-FT/IR analysis and gaseous products are primarily CO_2, CO, CH_4, H_2O, and a few organics [4]. It was studied TG-FT/IR coupling to monitor the pyrolysis products from some agricultural residues (coconut shell, sugarcane bagasse, corn stalks, and peanut shell) [5]. It was examined the influence of different pretreatments

on pyrolysis of agricultural residues such as wheat straw, olive residues, and peach stones and the main products of pyrolysis, CO_2, CO, CH_4, and H_2O were analyzed by means of an FT/IR. Also, he calculated the kinetic parameters using the distributed activation energy model [6]. It was reported the thermal degradation of orange peel was studied in dynamic air atmosphere by means of simultaneous TG-DSC and TG-FT/IR analysis. In general, this study suggests that the combustion reactions are controlled by the accessibility of the O_2 toward the vicinity of the residual solid, and during the two previous stages, the high release of H_2O, CO_2, CO, CH_4, and volatile organic compounds, apparently limits the O_2 accessibility and the reaction preferentially occur in gas phase [7]. It was reported that the biomass tar pyrolysis behavior was investigated in absence and presence of catalyst-dolomite with different heating rates. Different kinetic methods such as distributed activation energy model (DAEM), Coats&Redfern method were used to analyze the TG-DTA data to identify reaction parameters. It was found that the coexistence of dolomite greatly improved the amount and speed of tar pyrolysis process, and the calculation results of E_a also gave the quantity explanation [8]. In scientific investigation, the thermal behavior of the inner, the outer, and the mixture of inner and outer straw of coffee was carried out to evaluate the potential use of this material as biomass energy. The results showed the coffee straw as an important precursor, since it has a high enthalpy value (249.0 J g^{-1}) [9]. In addition to this, it were investigated the heat/mass transfer characteristics and nonisothermal drying kinetics at the first stage of biomass pyrolysis TG experiments of rice husk and cotton stalk were performed by a synchronic thermal analyzer (TG-DSC). It was found that the heat requirements for the dehydration of 1 kg rice husk and cotton stalk were 251 and 269 kJ, respectively [10]. It were reported the combustion properties and pyrolysis behavior of cigarette paper under the pyrolysis conditions of cigarette smoldering were investigated by micro-scale combustion calorimetry (MCC), thermogravimetric analysis coupled to Fourier transform infrared spectrometer (TG-FT/IR), respectively. The TG-FT/IR curves show that the pyrolysis process of cigarette paper mainly consists of four stages and the gaseous products are principally composed of CO_2, H_2O, CO, methanol, and carbonyl compounds [11].

Although there have been too many investigations about pyrolysis characteristics of different types of agricultural material, there are only a few studies on kinetic analysis especially about the devolatilization of sunflower, rice, corn, and wheat stalks based on Coats&Redfern, Horowitz&Metzger, and Arrhenius non-isothermal kinetic models. In the present study, devolatilization non-isothermal kinetic analysis of agricultural stalks and application of TG-FT/IR analysis were investigated. Stalks of agricultural materials, sunflower, rice, corn, and wheat, are abundant in Edirne in the Marmara Region which is important agricultural area in Turkey. Coats&Redfern, Horowitz&Metzger, and Arrhenius non-isothermal kinetic models were applied to calculate the devolatilization kinetic parameters and the devolatilization rate equations have been established. In addition to this, evolved gas analysis was examined in order to characterize the main compounds released during the devolatilization.

Experimental

Material and characterization

Sunflower, rice, corn, and wheat stalks were used as an agricultural material in this study. They chose because there are huge amounts of agricultural waste are easy to be obtained in Uzunköprü/Edirne in Marmara Region in Turkey. Natural dried agricultural stalks were grounded and reduced to <250 μm standard sieves (as determined by the American Society for Testing and Materials) before the characterization. Elemental analyses of the agricultural stalks were conducted in accordance with ASTM D3172-07a using a LECO CHN-600 carbon-hydrogen-nitrogen analyzer and the total sulfur content was determined by a LECO SC-132 sulfur analyzer (Table 1). The proximate analyses of the samples were performed in accordance with ASTM standard (ASTM E1131-03) and the calorific value was determined in accordance with ASTM D 5865-04 by a bomb calorimeter (IKA-Calorimeter C400) (Table 2). An average on three samples was taken for all mentioned analyses.

Table 1 Elemental analyses of the agriculture stalks

Stalk	C[a]/%	H[a]/%	N[a]/%	S[a]/%
Wheat	42.80	5.551	0.449	0.190
Rice	37.47	4.969	0.808	0.123
Corn	43.17	5.547	1.631	0.114
Sunflower	43.55	5.629	0.292	0.032

[a] On the dry basis

Table 2 Proximate analyses of the agriculture stalks

Stalk	Moisture/%	Ash/%	Volatile mater/%	Fixed carbon/%	Calorific values[a]/cal g^{-1}
Sunflower	8.42	2.06	87.36	2.16	3329
Rice	5.90	11.38	72.29	10.43	3200
Corn	8.80	8.78	78.76	3.66	3640
Wheat	6.13	3.20	86.87	3.80	3527

[a] On the dry basis

Crystallinity, infrared vibrational frequencies and microstructure of stalks were investigated by X-ray diffraction analysis (XRD), Fourier transform infrared spectroscopy (FT/IR), and scanning electron microscope (SEM), respectively.

Characterization techniques for structural analyses in the present study are listed below:

(1) XRD analysis: Crystallinity of stalks was determined by the XRD technique (Fig. 1). XRD analysis was carried out at an ambient temperature using a Philips Panalytical X'Pert-Pro diffractometer in a range of diffraction angle from 5° to 40° with CuKα radiation at operating parameters of 40 mA and 45 kV. The degree of crystallinity of cellulose is calculated based on the easy-to-use method of Segal as described in Eq. 1 [12–15].

$$\mathrm{CrI}\ (\%) = 100(I_{22} - I_{\mathrm{am}})/I_{22} \quad (1)$$

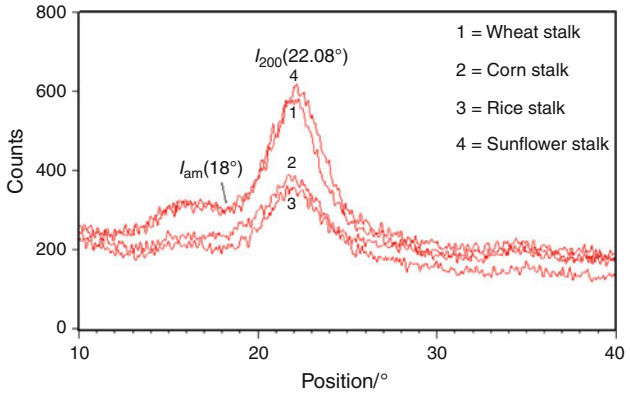

Fig. 1 XRD patterns of the agriculture stalks

where I_{am} is the intensity at amorphous peaks and I_{22} is the intensity at 2θ of 22.0°

(2) FT/IR analysis: Attenuated total reflectance (ATR) of FT/IR spectroscopy (Perkin Elmer Spectrum One) was used for determination the infrared vibrational frequencies. Before analysis, the crystal area was cleaned and the background reading collected; the material was placed over the small crystal area on a universal diamond ATR top-plate. Force was then applied to the sample, pushing it onto the diamond surface. The resulting FT/IR spectrum was recorded in the spectral range of 4000 to 650 cm^{-1} at ambient temperature; the resolution used was 4 cm^{-1} (Fig. 2).

(3) SEM analysis: The microstructure of the material was investigated by SEM (CamScan/Apollo300) analysis. The sample was made ready for analysis by fixing to the device's sample holder with the help of a carbon sticky band and coated with a small amount of conductive material, Au (Fig. 3).

Devolatilization and non-isothermal kinetic analysis

Devolatilization of stalks were carried out using the Perkin Elmer Diamond TG-DTA instrument, which was calibrated using of the melting points of indium ($T_{\mathrm{mp}} = 156.6$ °C) and tin ($T_{\mathrm{mp}} = 231.9$ °C) under the same conditions as the sample. The analyses were carried out at different heating rate of 10, 15, and 20 °C min^{-1} in atmosphere of N_2 that had a constant flow rate of 100 ml min^{-1}. The samples (~5 mg) were allowed to settle in standard alumina crucibles and heated up to 1000 °C. TG profiles at different heating rates are given in Fig. 4. TG system is coupling with FT/IR and time-base experiment can be performed to be analyzed the

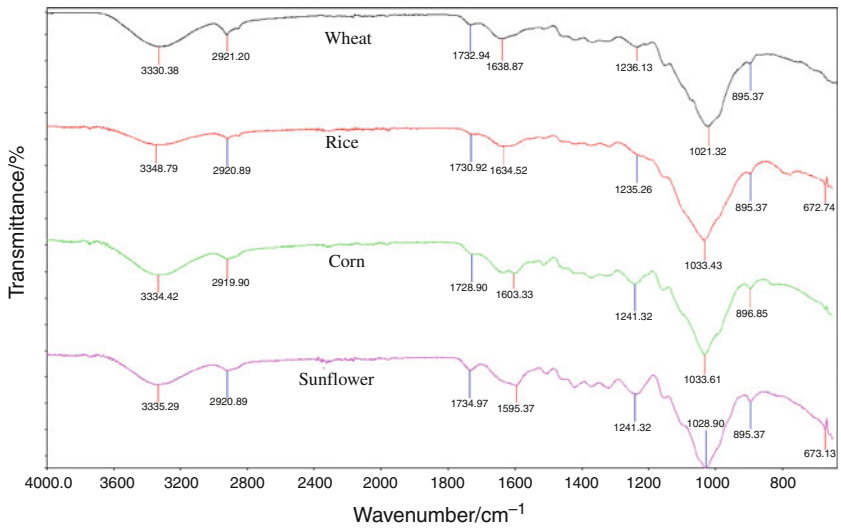

Fig. 2 FT/IR spectrums of the agriculture stalks

Table 3 Some fundamental frequencies of the agriculture stalks

Stalk	Band region/cm^{-1}					
	O–H	C–H	C=O	C=C	C–O	Bending vibrations
Sunflower	3335.29	2915.96	1734.97	1595.37	1033.61	894.10
Rice	3348.79	2915.96	1730.92	1634.52	1033.43	898.29
Corn	3334.42	2919.90	1728.90	1603.33	1033.61	896.85
Wheat	3330.38	2921.20	1732.94	1638.87	1021.32	984.10

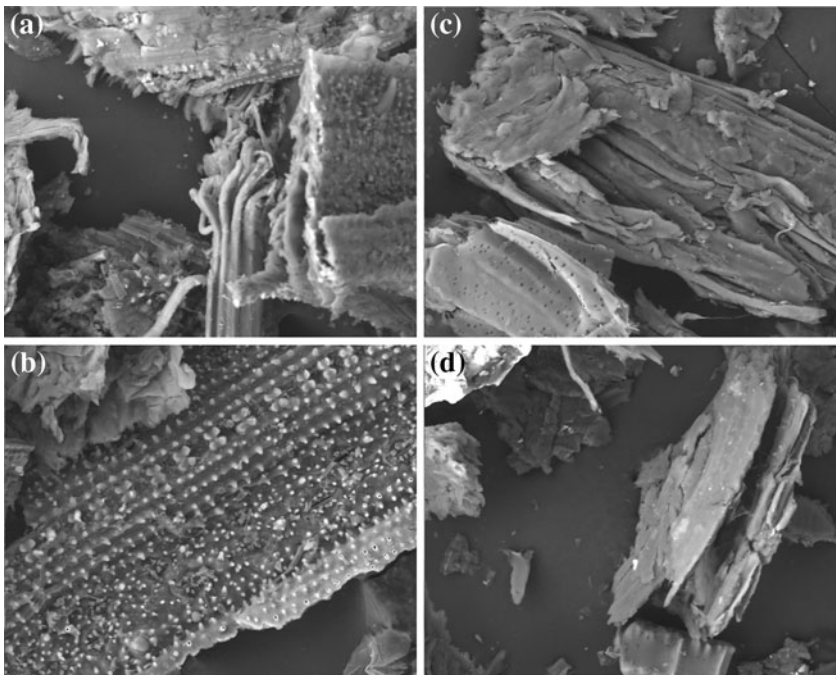

Fig. 3 SEM images of the agriculture stalks: **a** rice, **b** corn, **c** sunflower, **d** wheat

volatiles during the devolatilization (CH_4, H_2O, CO, CO_2, etc.). FT/IR stack plots of gas evolution determined in devolatization at different heating rate are given in Fig. 5.

In the present study, devolatilization reaction of the agricultural stalk samples can be defined as below:

$$\text{Agricultural stalk}_{(s)} \rightarrow \text{Volatiles}_{(g)} + \text{Char}_{(s)} \quad (2)$$

Kinetic analysis of devolatilization reactions of agricultural stalk were investigated by using mathematical equations of Coats&Redfern, Horowitz&Metzger, and Arrhenius non-isothermal kinetic models based on multiply heating rates.

According to the Coats&Redfern method, values of $[\log(-\log(1-\alpha)/T^2)]$ versus $1/T$ was plotted. The slope of the line was used to calculate activation energy (E_a) and also pre-exponential factor (k_0) was determined from the intercept of the line (Eqs. 3 and 4). In this method, $1/T$ should give a straight line with a correlation coefficient (R^2) for a corrected value of order of the reaction (n). In the Coats&Redfern method, reaction orders were assumed to have the values from 0 to 3 in the decomposition fraction (α) range from 0.1 to 0.9 [16].

$$\log\left[\frac{1-(1-\alpha)^{1-n}}{T^2(1-n)}\right] = \log\frac{k_0R}{\beta E_a}\left[1-\frac{2RT}{E_a}\right] - \frac{E_a}{2.303RT} \quad \text{for } n \neq 1 \quad (3)$$

$$\log\left[\frac{-\log(1-\alpha)}{T^2}\right] = \log\frac{k_0R}{\beta E_a}\left[1-\frac{2RT}{E}\right] - \frac{E_a}{2.303RT} \quad \text{for } n = 1 \quad (4)$$

In the Horowitz&Metzger method, reaction order is assumed to 1. The calculation of kinetic parameters was made based on Eq. 5. A plot of $\ln[(W_o - W)/(W_o - W_f)]$ against θ was drawn which gave straight lines in all the cases with the slope $E_a/2.303RT_m^2$ from which E_a values were obtained [17].

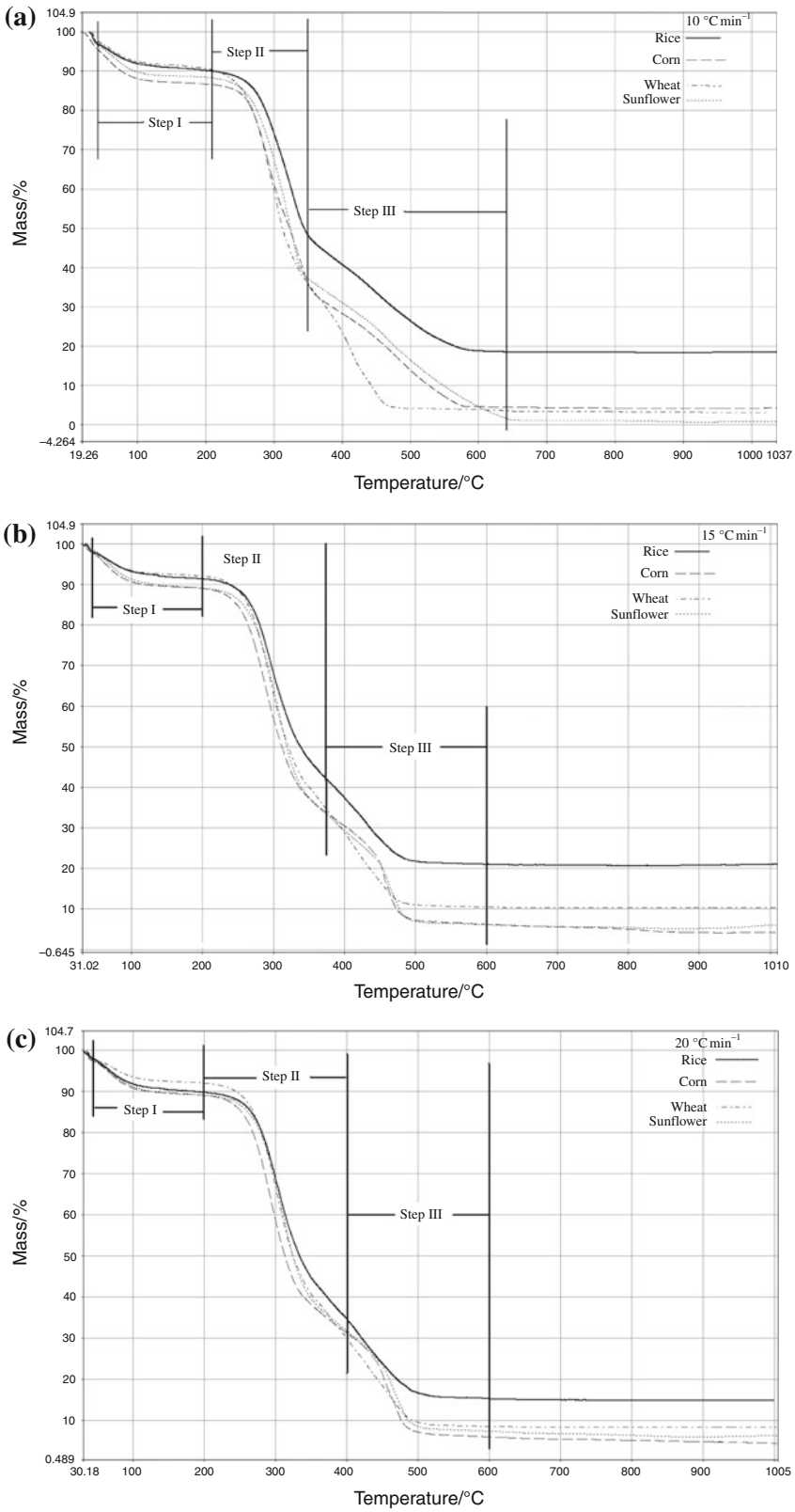

Fig. 4 TG profiles of devolatization of the agriculture stalks at different heating rates: **a** 10 °C min^{-1}, **b** 15 °C min^{-1}, **c** 20 °C min^{-1}

Table 4 Characteristic temperatures of devolatization reactions of the agriculture stalks

β/°C min^{-1}	Stalk	Step	T_i/°C	T_m/°C	T_f/°C	R_m/%min^{-1}
10	Sunflower	II	187.28	316.13	366.77	10.89
		III	366.77	452.97	661.96	1.89
	Rice	II	142.72	326.92	395.31	7.64
		III	395.31	445.47	613.25	1.62
	Corn	II	195.38	290.85	372.42	8.16
		III	401.15	480.87	577.27	1.78
	Wheat	II	166.72	295.65	359.21	11.49
		III	360.11	406.60	485.45	3.86
15	Sunflower	II	214.01	307.27	373.00	16.31
		III	420.08	455.65	521.34	7.33
	Rice	II	181.87	300.86	398.70	12.41
		III	398.80	427.78	615.52	3.50
	Corn	II	200.37	289.41	383.80	14.25
		III	413.19	451.48	590.39	8.12
	Wheat	II	178.11	288.52	380.24	15.47
		III	380.24	450.59	545.87	3.91
20	Sunflower	II	223.21	310.29	373.79	20.53
		III	422.01	457.20	539.01	8.86
	Rice	II	187.40	305.03	395.15	16.88
		III	396.53	432.99	640.05	4.25
	Corn	II	238.37	293.71	377.40	21.04
		III	403.69	446.57	607.74	9.63
	Wheat	II	195.75	303.26	401.19	21.21
		III	401.87	445.02	562.80	4.75

$$\ln\left[\frac{W_o - W}{W_o - W_f}\right] = \frac{E_\alpha \theta}{RT_m^2} \quad (5)$$

In the Arrhenius method (Eq. 6), the rate of mass loss of the total sample depends only on the rate constant, the mass of sample remaining and the temperature and reaction order is assumed to 1. E_a is calculated from the slope, and k_0 can be determined from the intercept [18].

$$\frac{dW}{dt} = k_0 \times \exp\left(\frac{-E_a}{RT}\right) \times W \quad (6)$$

The literature has indicated that the activation energy depends on several parameters such as heating rate, particle size distribution, atmosphere and crucible type, etc. It has been accepted that under different experimental conditions, between the logarithm of the pre-exponential factor ($\ln k_0$) and the apparent activation energy (E_a) is observed a linear relationship which is known as kinetic compensation effect (KCE). KCE means that the reduction in rate expected to result from an increase in E_a due to a compensatory increase of k_0. The KCE was evaluated in order to validate the kinetic data [19–22].

Results and discussion

Crystallinity, infrared vibrational frequencies, and microstructure of stalks

Structurally agricultural materials on average, contains of lignin (15–25%), cellulose (38–50%), hemicellulose (23–32%), some proteins and apparent moisture. Crystallinity, infrared vibrational frequencies, and microstructure of stalks were investigated by XRD, FT/IR, and SEM, respectively, in this study.

The crystallinity was calculated from XRD patterns of the agricultural stalks in the diffraction range 10°–40° shown in Fig. 1. As can be seen, two peaks appeared at about 2θ of 18.0° and 22.0° and the four stalks showed the similar diffraction profile. The bigger one was the major peak representing the crystalline cellulose structure and the smaller one was a secondary peak representing the amorphous cellulose structure in the agricultural stalks. Cellulose is the complex polymer with crystalline and amorphous areas. The crystallinity of cellulose was calculated as 42.11% for rice, 46.84% for corn, 40.96%

Table 5 Kinetic parameters calculated from Coats&Redfern model

β/°C min^{-1}	Stalk	Step	n	E_a/kJ mol^{-1}	k_o/min^{-1}	R^2
10	Sunflower	II	0.74	94.01	5.86×10^{7}	0.9987
		III	1.73	75.52	2.06×10^{4}	0.9978
	Rice	II	1.45	105.23	7.65×10^{8}	0.9994
		III	2.04	124.93	1.46×10^{8}	0.9960
	Corn	II	1.91	119.76	2.69×10^{10}	0.9920
		III	1.72	121.58	5.53×10^{7}	0.9971
	Wheat	II	1.00	86.95	2.01×10^{7}	0.9980
		III	1.74	170.09	3.48×10^{12}	0.9982
15	Sunflower	II	1.58	124.65	1.11×10^{11}	0.9998
		III	0.91	253.70	5.98×10^{17}	0.9982
	Rice	II	2.50	131.98	6.58×10^{11}	0.9989
		III	2.56	313.77	8.14×10^{22}	0.9961
	Corn	II	2.20	132.74	1.30×10^{12}	0.9999
		III	1.35	267.75	6.39×10^{20}	0.9935
	Wheat	II	2.21	131.02	8.82×10^{11}	0.9997
		III	1.90	186.06	6.61×10^{13}	0.9938
20	Sunflower	II	1.58	130.57	4.36×10^{11}	0.9998
		III	1.10	255.87	1.09×10^{18}	0.9996
	Rice	II	2.52	142.31	7.09×10^{12}	0.9998
		III	2.21	202.04	5.49×10^{14}	0.9951
	Corn	II	2.50	172.29	9.73×10^{15}	0.9997
		III	1.20	226.30	1.22×10^{16}	0.9990
	Wheat	II	2.90	149.79	3.42×10^{13}	0.9990
		III	1.70	193.84	9.29×10^{13}	0.9934

for sunflower and 42.78% for wheat stalks based on Eq. 1.

Figure 2 represents the FT/IR spectra and the fundamental peaks of the studied agricultural stalk are listed in Table 3. FT/IR spectra of the rice, corn, sunflower, and wheat stalk used to determine the vibration frequency in the functional groups. Generally, the peaks observed at about 3300 cm^{-1} can be assigned to existence of free and intermolecular bonded hydroxyl groups. The absorption peak around 2900 cm^{-1} indicates the stretching vibration of C–H band. The peak at around 1700 cm^{-1} is due to C=O band vibration and the peak at 1600 cm^{-1} is corresponds to the C=C stretching relevant with lignin aromatic groups. The strong band at around 1033 cm^{-1} is due to –OCH_3 group confirms the presence of lignin in the samples. Also, the peak at around 890 cm^{-1} is assigned to the bending modes of aromatic compounds [23]. SEM is used to observe visually the physical and microstructure in the agricultural stalk. SEM images at 500× magnification of the stalks shown in Fig. 3.

Devolatilization and kinetic analysis

Thermogravimetric profiles at different heating rates of the devolatilization of the agricultural stalks are given in Fig. 4 and Table 4 gives data obtained through interpretation of these profiles. Considering each agricultural stalks, the profile of TG curves are exhibit a similar devolatilization behavior. It can be seen that the devolatilization of agricultural stalk can be divided into three steps such as initial (Step I), main devolatilization (Step 2) and slight devolatilization (Step 3). For all stalks, the main devolatilization stage started slowly after moisture evaporation and increased sharply. Moisture evaporation was occurred at the initial step in the temperature ranges 37.88–133.54 °C for sunflower stalk, 38.77–119.93 °C for rice stalk, 37.80–130.49 °C for corn stalk and 39.59–141.66 °C for wheat stalk. No significant difference in the temperature range in the initial step for the stalks. Main devolatilization of studied stalks starts at around 140–190 °C temperature depending on the biomass structure and the volatiles releasing rate increases and temperature

Table 6 Kinetic parameters calculated from Horowitz&Metzger model

β/°C min^{-1}	Stalk	Step	E_a/kJ mol^{-1}	R^2
10	Sunflower	II	79.61	0.9915
		III	40.64	0.9544
	Rice	II	73.08	0.9827
		III	56.57	0.9544
	Corn	II	63.24	0.9430
		III	68.35	0.9690
	Wheat	II	71.08	0.9780
		III	93.14	0.9659
15	Sunflower	II	121.10	0.9782
		III	121.61	0.9509
	Rice	II	52.68	0.8776
		III	111.62	0.8844
	Corn	II	62.08	0.9079
		III	175.19	0.9454
	Wheat	II	59.91	0.9079
		III	150.37	0.9655
20	Sunflower	II	109.97	0.9917
		III	229.10	0.9694
	Rice	II	58.95	0.8956
		III	85.95	0.8945
	Corn	II	68.42	0.9064
		III	151.20	0.9655
	Wheat	II	51.58	0.8676
		III	108.43	0.9303

Table 7 Kinetic parameters calculated from Arrhenius model

β/°C min^{-1}	Stalk	Step	E_a/kJ mol^{-1}	k_o/min^{-1}	R^2
10	Sunflower	II	97.74	1.02×10^8	0.9976
		III	36.24	0.26×10^2	0.9634
	Rice	II	89.55	10.88×10^6	0.9890
		III	19.37	0.11×10^1	0.8253
	Corn	II	113.37	4.19×10^9	0.9787
		III	40.51	0.58×10^2	0.9801
	Wheat	II	95.81	11.85×10^7	0.9801
		III	61.74	8.1×10^3	0.9794
15	Sunflower	II	107.18	0.95×10^4	0.9963
		III	188.36	0.49×10^6	0.9689
	Rice	II	94.20	0.25×10^4	0.9829
		III	115.97	0.14×10^5	0.7184
	Corn	II	109.99	0.15×10^5	0.9953
		III	184.07	0.39×10^6	0.9730
	Wheat	II	105.29	0.88×10^4	0.9969
		III	30.76	0.46×10^1	0.9678
20	Sunflower	II	108.88	0.11×10^5	0.9976
		III	155.39	0.48×10^5	0.9626
	Rice	II	90.52	0.18×10^4	0.9682
		III	16.35	1.48	0.7966
	Corn	II	109.21	0.15×10^5	0.9926
		III	159.24	0.74×10^5	0.9605
	Wheat	II	109.48	0.13×10^5	0.9976
		III	40.36	0.10×10^1	0.9938

reach to about 360–390 °C. After further heating over the 400 °C the slight devolatilization was stared and continues up to the 650 °C. It is well known from the literature cellulose, hemicelluloses, and lignin degrade in several steps. The differences in the temperature are due to the variations in stalks compositions. Generally, during the second step of the devolatilization decomposition of the cellulose and hemicelluloses was occurred and afterwards lignin and decomposition of remaining cellulose and hemicelluloses was occurred at the third step. It is not possible to separate the different devolatilization steps because the reactions are very complex.

Heating rate has significant effect on the devolatilization of agricultural stalks. The increase of the heating rate leads to a less uniform heat distribution and a higher temperature gradient. It can be seen that all characteristic temperatures were shifted to higher values with increasing heating rate. The devolatilization temperatures (T_i and T_f), the reaction rates (R_m) and the temperature at which the maximum weight loss occurred (T_m) all increased at main devolatilization and slight devolatilization steps.

Kinetic study of main and slight devolatilization reactions were investigated based on the Coats&Redfern, Horowitz&Metzger and Arrhenius models. In the Coats&Redfern model, E_a and k_o was calculated, after the determination of the corrected value of n, from the slope and the intercept of the kinetic plots for the step II and III. According to the Table 5, the activation energy values changes with changes in heating rate and exhibited the same behavior in step II and III for all agricultural stalks. Activation energy showed a continuous increase with increasing heating rate from 10 to 20 °C min^{-1}. Average of the activation energy was used to compare the results of different agricultural stalks. The average activation energy of step II was calculated as 116.41, 126.50, 141.59, and 122.58 kJ mol^{-1} for sunflower stalk, rice stalk, corn stalk, and wheat stalk, respectively. The average activation energy of different agricultural stalks for step II is closed with each other. For step III, the average activation energy was calculated as 195.03, 213.31, 205.21, and 183.33 kJ mol^{-1} for sunflower stalk, rice stalk, corn stalk, and wheat stalk, respectively. Based on these results, it can be clearly said that the activation energy of step III was always higher than the step II. This is the expected result because of thermal degradation of lignin was occurred at step III. It known that lignin decomposes slower, over a

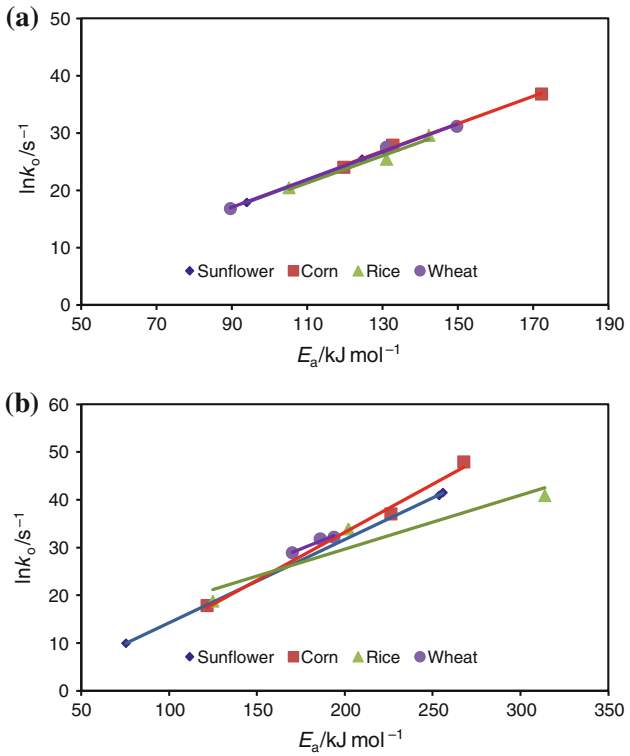

Fig. 5 Kinetic compensation effect plots for the Coats&Redfern method: **a** Step II, **b** Step III

Table 8 Kinetic compensation effects plot equations and R^2 values for Coats&Redfern method

Stalk	Step	Equation	R^2
Sunflower	II	$y = 0.2446x - 5.1048$	0.9999
	III	$y = 0.1746x - 3.2549$	0.9999
Rice	II	$y = 0.249x - 5.6684$	0.9979
	III	$y = 0.179x - 3.0647$	0.9981
Corn	II	$y = 0.2394x - 4.3256$	0.9963
	III	$y = 0.2014x - 7.0777$	0.9926
Wheat	II	$y = 0.2309x - 3.1379$	0.9978
	III	$y = 0.1451x + 4.3452$	0.9468

broader temperature range than cellulose and the hemicellulose and have different thermal stabilities because various oxygen functional groups [24].

In addition, as an example of the rate equations of the devolatilization reactions can be written for the wheat stalk. Rate equations can be written for the other stalks as similar equations in Eqs. 7 and 8.

$$\text{Step II:} \quad \frac{d\alpha}{dt} = 2.01 \times 10^{7} e^{-8695/RT} (1-\alpha)^{1.00} \tag{5}$$

$$\text{Step III:} \quad \frac{d\alpha}{dt} = 3.48 \times 10^{12} e^{-(17009/RT)} (1-\alpha)^{1.74} \tag{6}$$

In the Horowitz&Metzger model, E_a assume that intermediates are not formed, that degradation products escape immediately, and that the nature of the reaction (E_a, A, n, k) does not change in the temperature range of interest. Table 6 shows E_a values for two steps of the devolatilization of the four stalks. The activation energy values calculated by Horowitz&Metzger method does not exhibited the same behavior with the changes in heating rate compared with Coats&Redfern. Increase with the increase of heating rate was observed in some cases, were sometimes reduced and it can be seen that the lower R^2 values was obtained. However, it is noted that Horowitz&Metzger model is more appropriate in a narrow temperature range and the R^2 was highest for the Coats&Redfern ($\sim$0.99) method than Horowitz&Metzger. Thus, it will be more accurate to compare the results based on average activation energy obtained from Horowitz&Metzger and Coats&Redfern. The average activation energy of step II was calculated as 103.56, 61.57, 64.58, and 60.85 kJ mol^{-1} for sunflower stalk, rice stalk, corn stalk, and wheat stalk, respectively. For step III, the average activation energy was calculated as 130.45, 84.71, 131.58, and 117.30 kJ mol^{-1} for sunflower stalk, rice stalk, corn stalk, and wheat stalk, respectively. For all that based on Horowitz&Metzger kinetic model, it was found that the activation energy of step III was still higher than the step II as expected. In the Arrhenius model, E_a and k_o was calculated assumes that the rate of mass loss of the total sample is dependent only on the rate constant and the mass of sample reaming. Lower R^2 values were obtained based on the Arrhenius model. The results are not compatible obtained by Arrhenius and Coats–Redfern methods. The average activation energy of step II was calculated as 104.60, 93.09, 110.85, and 103.52 kJ mol^{-1} for sunflower stalk, rice stalk, corn stalk, and wheat stalk, respectively. For step III, the average activation energy was calculated as 279.93, 50.56, 127.94, and 44.28 kJ mol^{-1} for sunflower stalk, rice stalk, corn stalk, and wheat stalk, respectively (Table 7).

As a result of non-isothermal kinetic analysis, Coats–Redfern method best represent the step II and step III devolatilization reaction of agricultural stalks. In order to validate the kinetic data reported in the case of the Coats–Redfern, KCE was applied. The KCE plots of E_a against to the lnk_0 values for each heating rates give in Fig. 5 and plot equation of the KCE with R^2 are present at Table 8. As can be seen, kinetic data of step II and step III devolatilization reaction of agricultural stalks exhibit the KCE with high correlation coefficient. Thus, pre-exponential factor and activation energy exhibited the same behavior when the heating rate was changed.

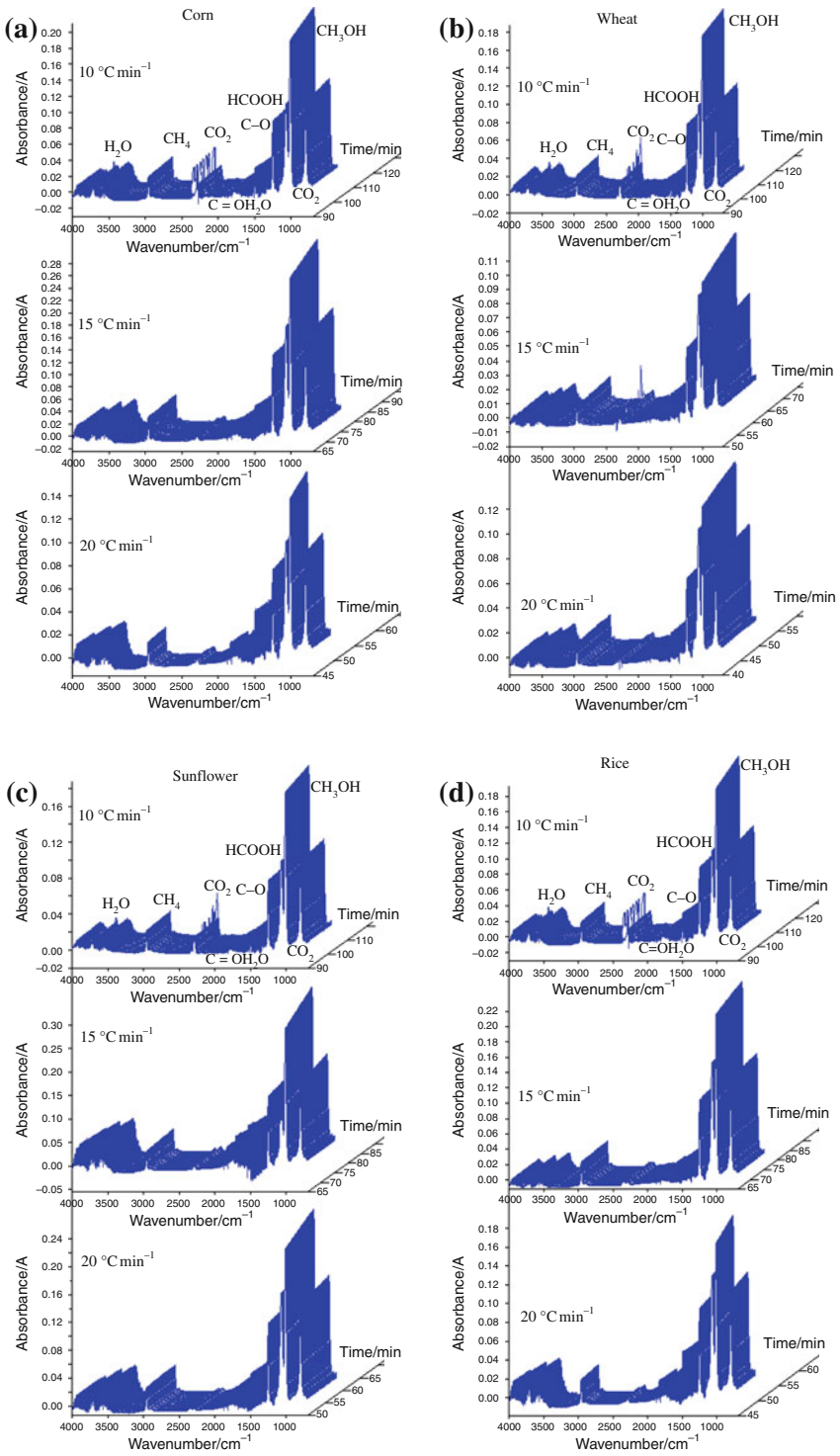

Fig. 6 FT/IR stack plots of devolatization of the agriculture stalks at different heating rate: **a** corn, **b** wheat, **c** sunflower, **d** rice

Application of TG-FT/IR analysis

Figure 6 shows the FT/IR stack plot taken during the devolatilization of the agricultural stalks at different heating rates. Several gas products were evolved at same time and the stack plot contains the sums of the spectral signature. Qualitative analysis was performed based on region and the peak positions. During the devolatilization of biomasses, gases (CH_4, CO, CO_2, H_2O, CH_3OH, HCOOH and some organics) can be easily detected in the specific wavenumber. Some characteristic wave numbers of gas species: H_2O (4000–3400 cm^{-1}, 1550–1350 cm^{-1}); CH_4 (3000–2800 cm^{-1}, 1400–1360 cm^{-1}); CO_2 (2400–2250 cm^{-1}, 680–660 cm^{-1}), CO (2200–2000 cm^{-1}) C=O bond of esters,

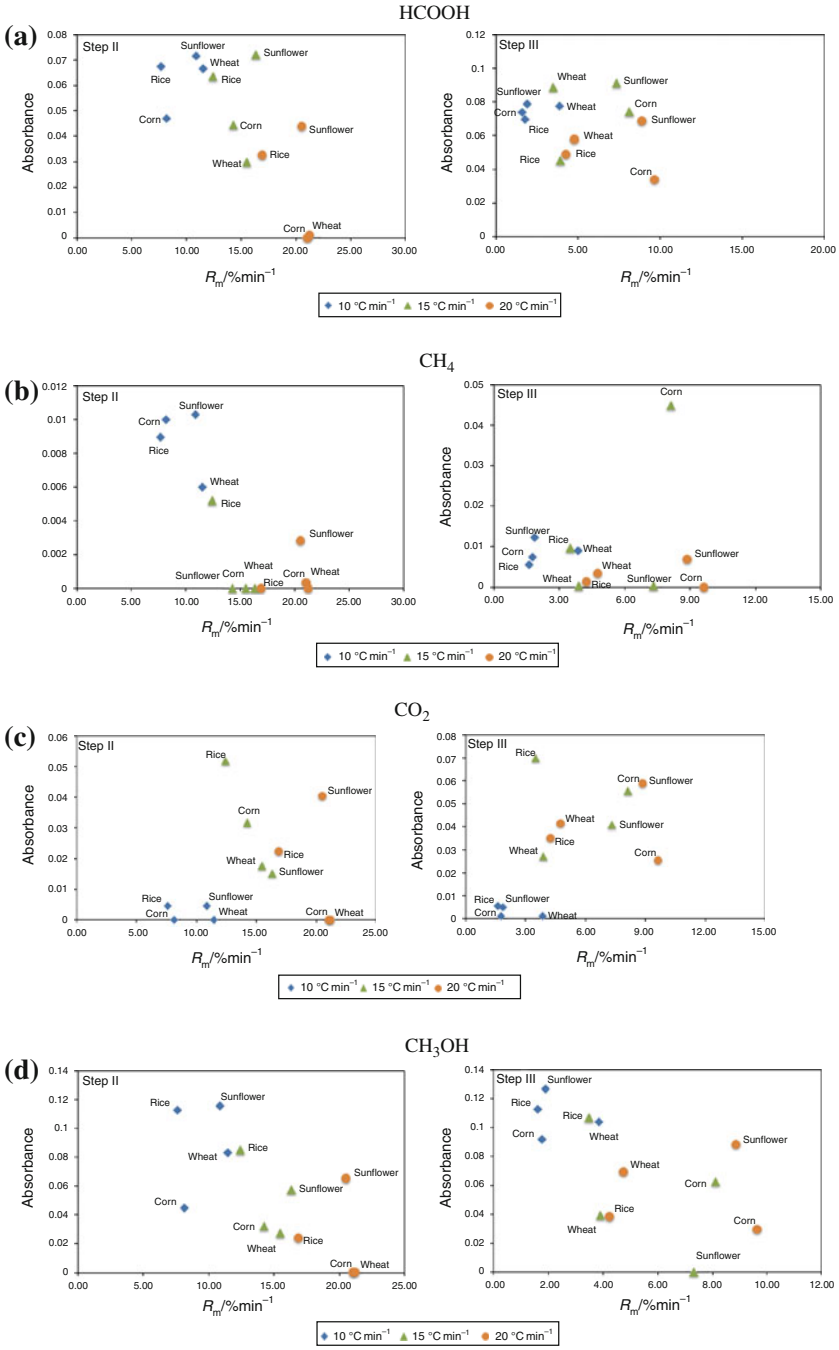

Fig. 7 Gas evolution determined via TG-FT/IR in devolatization at different heating rate: **a** HCOOH, **b** CH_4, **c** CO_2, **d** CH_3OH

aldehydes, and ketones (1660–1820 cm^{-1}), C–O bond of an unsaturated carbon (1280–1260 cm^{-1}).

Figure 7 shows the IR absorbance of CH_4, CO_2, HCOOH, and CH_3OH as a maximum devolatilization rate of Step II and III at different heating rates. Considering each agricultural stalks, the profile of stalk plots are very similar indicating that all exhibit a similar devolatilization behavior. Comparing themselves the agricultural stalks, the spectra for each one was taken from the rate of most intense mass loss and the time scale can correspond to the devolatilization temperature. Amount of gasses was evaluated based on Beer's Law which assumes that the absorbance of the components is directly proportional to their concentrations. The gaseous products are evolved in a much narrower range of time as heating rate increase for all the agricultural stalks. It is also noted that maximum devolatilization appeared to increase with an increase in heating rate. Based on the results of evolution determined

at step II for all the agricultural stalks, it can be said that as heating rates increase the release of HCOOH, CH_4, and CH_3 is mainly decrease. However, the release of CO_2 in this stage is increase with increasing heating rate from 10 to 20 °C min^{-1}. This indicated that, the increase of release amount of CO_2 is mainly caused by the conversion of HCOOH, CH_4, and CH_3 to the CO_2 in the main devolatilization step. Sunflower has a relatively large CO_2 peak compared with other stalks. When devolatilization progresses into the slight step, a small quantity of volatiles are released. From all the gaseous evolution results obtained at step III, it is demonstrated that conversion of gases to each other are more randomly, and there is no any rule based effect on heating rate changing on gases amount release.

Conclusions

In this study, devolatilization behavior of several types of agricultural stalks (sunflower, rice, corn, and wheat) was studied using thermogravimetric system (TG) under nitrogen atmosphere at different heating rates (10, 15, and 20 °C/min). Coats&Redfern, Horowitz&Metzger, and Arrhenius non-isothermal kinetic models were applied to calculate the devolatilization kinetic parameters. The following points result from this study:

(1) There are no significant differences in the devolatilization characteristic for the same type agricultural stalks include lignin, cellulose, and hemicellulose. Total mass loss at step II and step III was determined as 78.946, 66.39, 69.96, and 80.74% for sunflower, rice, corn and wheat, respectively. Base on this results, agricultural stalks seem to be best option for the production of gas to be used as a fuel directly by devolatilization process.

(2) The results obtained from three different models were compared the Horowitz&Metzger and Arrhenius methods did not give as close of an agreement compared to Coats&Redfern. As the structure characteristic (chemical composition, crystallinity, etc.) of the stalk, the kinetic parameters were found to be different. The average activation energy of step II was calculated as 116.41, 126.50, 141.59, and 122.58 kJ mol^{-1} for sunflower stalk, rice stalk, corn stalk, and wheat stalk, respectively. For step III, the average activation energy was calculated as 195.03, 213.31, 205.21, and 183.33 kJ mol^{-1} for sunflower stalk, rice stalk, corn stalk, and wheat stalk, respectively. In order to validate the kinetic data reported in the case of the Coats–Redfern, KCE was applied and KCE is accepted. Thus, pre-exponential factor and activation energy exhibited the same behavior when the heating rate was changed.

(3) XRD results indicated that there was a relationship between the degree of crystallinity and the activation energy value, higher crystallinity values standing together with higher E_a values. The higher value of crystallinity of the corn stalk can be due to higher E_a value of stage II where devolatilization decomposition of the cellulose and hemicelluloses was occurred.

According to the TG-FT/IR analysis, devolatilization gases (CH_4, CO_2, H_2O, CH_3OH, HCOOH) was detected and the amount of selected gases was evaluated based on IR absorbance value function to the maximum devolatilization rate. It is found that sunflower released the maximum total amount of gases (CH_4, CO_2, HCOOH, and CH_3OH) compared with other stalks and this result accordance with the proximate analyses. In addition to this, release of CO_2 from sunflower is relatively higher compared with other agricultural stalks.

References

1. Tonbul Y. Pyrolysis of pistachio shell as a biomass. J Therm Anal Calorim. 2008;91(2):641–7.
2. Buryan P, Staff M. Pyrolysis of the waste biomass. J Therm Anal Calorim. 2008;93(2):637–40.
3. Bassilakis R, Carangelo RM, Wójtowicz MA. TG-FTIR analysis of biomass pyrolysis. Fuel. 2001;80(12):1765–86.
4. Yang H, Yan R, Chin T, Liang DT, Chen H, Zheng C. Thermogravimetric analysis-fourier transform infrared analysis of palm oil waste pyrolysis. Energ Fuel. 2004;18:1814–21.
5. Souza S, Moreira P, Teixeira A. TG-FTIR coupling to monitor the pyrolysis products from agricultural residues. J Therm Anal Calorim. 2009;97:637–42.
6. Giuntoli J, Arvelakis S, Spliethoff H, Jong W, Verkooijen A, H M. Quantitative and kinetic thermogravimetric Fourier transform infrared (TG-FTIR) study of pyrolysis of agricultural residues: influence of different pretreatments. Energ Fuel. 2009;23:5695–706.
7. Zapata B, Balmaseda J, Fregoso-Israel E, Torres-Garcia E. Thermo-kinetics study of orange peel in air. J Therm Anal Calorim. 2009;98:309–15.
8. Li C, Suzuki K. Kinetic analyses of biomass tar pyrolysis using the distributed activation energy model by TG/DTA technique. J Therm Anal Calorim. 2009;98:261–6.
9. Orsini R, Filho M, Mercuri L, Matos J, Carvalho F. Thermoanalytical study of inner and outer residue of coffee harvest applications on biomass. J Therm Anal Calorim. 2011. doi:10.1007/s10973-011-1542-5.
10. Chen D, Zhang D, Zhu X. Heat/mass transfer characteristics and nonisothermal drying kinetics at the first stage of biomass pyrolysis. J Therm Anal Calorim. 2011. doi:10.1007/s10973-011-1790-4.
11. Zhou S, Wang C, Xu Y, Hu Y. The pyrolysis of cigarette paper under the conditions that simulate cigarette smouldering and puffing. J Therm Anal Calorim. 2011;104:1097–106.
12. He Y, Pang Y, Liu Y, Li X, Wang K. Physicochemical characterization of rice straw pretreated with sodium hydroxide in the

solid state for enhancing biogas production. Energ Fuel. 2008;22: 2775–81.
13. Niu K, Chen P, Zhang X, Tan WS. Enhanced enzymatic hydrolysis of rice straw pretreated by alkali assisted with photocatalysis technology. J Chem Technol Biotechnol. 2009;84:1240–5.
14. Corradini E, Teixeira M, Paladin D, Agnelli A, Silva F, Mattoso C. Thermal stability and degradation kinetic study of white and colored cotton fibers by thermogravimetric analysis. J Therm Anal Calorim. 2009;97(2):415–9.
15. Bansal P, Hall M, Realff MJ, Lee JH, Bommarius AS. Multivariate statistical analysis of X-ray data from cellulose: a new method to determine degree of crystallinity and predict hydrolysis rates. Bioresource Technol. 2010;101:4461–71.
16. Coats AW, Redfern JP. Kinetic parameters from thermogravimetric data. Nature. 1964;201:68–9.
17. Horowitz HH, Metzger G. A new analysis of thermogravimetric traces. Anal Chem. 1963;35(10):1464–8.
18. Elbeyli I, Piskin S, Sutcu H. Pyrolysis kinetics of Turkish bituminous coals by thermal analysis. Turk J Eng Environ Sci. 2004; 28:233–9.
19. Brown ME, Maciejewskib M, Vyazovkinc S, Nomend R, Sempered J, Burnhame A, Opfermannf J, Streyg R, Andersong HL, Kemmlerg A, Keuleersh R, Janssensh J, Desseynh HO, Lii C, Tangi T, Roduitj B, Malekk J, Mitsuhashi T. Computational aspects of kinetic analysis part A: the ICTAC kinetics project-data, methods and results. Thermochim Acta. 2000;355:125–43.
20. Dantas MB, Almeida AAF, Concei MM, Fernandes VJ Jr, Santos MG, Silva FC, Soledade LEB, Souza AG. Characterization and kinetic compensation effect of corn biodiesel. J Therm Anal Calorim. 2007;87(3):847–51.
21. Dias DS, Crespi MS, Ribeiro CA, Fernandes JLS, Cerqueira HMG. Application of non-isothermal cure kinetics on the interaction of poly(ethylene terephthalate)-alkyd resin paints. J Therm Anal Calorim. 2008;91(2):409–12.
22. Vyazovkina S, Burnhamb AK, Criadoc JM, Pérez-Maquedac LA, Popescud C, Sbirrazzuolie N. ICTAC kinetics committee recommendations for performing kinetic computations on thermal analysis data. Thermochim Acta. 2011;520:1–19.
23. Garg UK, Kaur MP, Garg VK, Sud D. Removal of hexavalant chromium from aqueous solution by agricultural waste biomass. J Hazard Mater. 2007;140:60–8.
24. Brebu M, Vasile C. Thermal degradation of lignin. Cellul Chem Technol. 2010;44(9):353–63.